Three dimensional strain and temperature monitoring of composite laminates.

Geert Luyckx, Wim De Waele, Joris Degrieck, Wim Van Paepegem
Ghent University, St-pietersnieuwstraat 41 9000 Ghent
Johan Vlekken, Stephan Vandamme
FOS&S, Cypalstraat 14, 1440 Geel
Karima Chah
VUB, Pleinlaan 2, 1050 Elesene

Abstract

This paper discusses a new sensor design based on optical fibre Bragg gratings which is being developed in the framework of the MASSFOS-project ('Multi-Axial Stress and Strain sensing of thermo hardened composite elements using Fibre Optic Sensors'-project). The main technical objective of this ESA co-funded project is the development of a monitoring system which measures dynamically the multi-axial stress and strain in thermo hardened composite elements (made of space qualified material). The sensor consists of a 'High Birefringence'-fibre (HiBi-fibre) in which two gratings are inscribed; each grating yields two distinct Bragg peaks. The first grating is sensitive to the total stress field in the material, while the second one is isolated from transverse stress components. By measuring the four Bragg peaks of the sensor, it is possible to determine the total strain field, plus the temperature inside a composite material. Theoretical simulations have indicated a good strain resolution of the proposed design. Experimental calibration of the sensor gave similar results.

Keywords
Fibre Bragg sensors, Multi-axial stress/strain monitoring, Thermo-hardened composite elements.

Introduction

An increasing use of composite materials in structures can be noticed over the last few decades, because of the possible weight savings and their high specific stiffness and strength. Although the manufacturing process of these materials is still very labour intensive, it allows the integration of sensors (e.g. fibre optics) which can online register the mechanical behaviour of the structural component. Other inspection techniques like visual surveillance, ultrasonic inspection, and radiography require highly educated personnel for the interpretation of the resulting data and even lack the possibility to collect data between two inspection intervals.
Two aspects can motivate the design of an on-line monitoring system able to measure the total strain field (plus temperature) inside a composite structure. The first one can be situated in the area of damage detection. Existing design guidelines for (complex) composite structures are sometimes based on subjective information about structural

condition coupled with untested or, worse, invalid assumptions about material behaviour and performance and their relationship to damage, deterioration and defects [1].
The second aspect is the existence of residual stresses after the curing of composite materials. A sensor able to monitor the total strain/stress field of a composite laminate could be helpful to analyze these stresses, both quantitatively and qualitatively. This leads to an optimization of the design of a certain structure and the production process. One thing is sure, measuring only the axial strain will not be sufficient to judge about the health condition of a structure.
The possibility of monitoring the condition of an in-service structure should certainly elucidate these matters, and should greatly enhance the insight and confidence in the (long-term) behaviour of composite structures. The feedback from recorded loads, deformations and temperatures of (parts of) existing structures in real conditions, can lead to very valuable information for design conditions, or even to the adaptation of current standards and rules.

In the MASSFOS-project [2], the authors try to measure dynamically the total strain field plus the temperature by developing a monitoring system based on optical fibre Bragg gratings. The project focuses on the integration of the sensors, the development of an interrogation system and production and testing on composite test samples. The objective is to make on-line health monitoring of carbon composites possible. This paper discusses on the new sensor design which will be developed during the project. Firstly, a short review is given on axial as well as multi-axial fibre Bragg gratings. Secondly the new sensor will be presented with some theoretical and experimental results.

Fibre Bragg gratings: 'From Uni-axial to Multi-axial sensing technique'

General principle

Fibre Bragg Gratings (FBGs) can be considered as the optical counterpart of classical strain gauges. When a broadband light spectrum is coupled into the fibre in which a Fibre Bragg grating (FBG) is written, only a narrow part of the spectrum will be back reflected. This spectrum is centered on the Bragg-wavelength λ_B (see Figure 1).

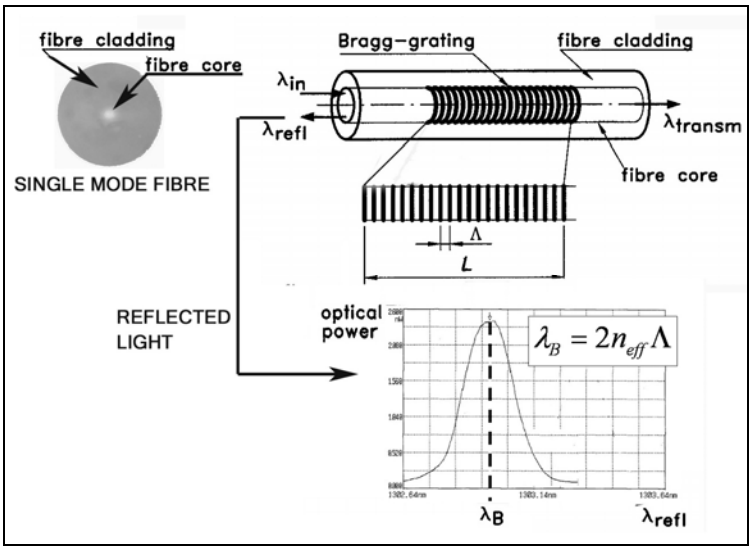

Figure 1 Schematic representation of a Bragg-grating in an optical fibre, with the planes of the modulated index of refraction. Also shown is the typical spectral response from such a grating inscribed in a single-mode fibre after in-coupling of light of a broadband light source.

The central wavelength of this reflected spectrum (the Bragg wavelength) shifts as a function of the elongation or shortening of the fibre and temperature changes. Spectral analysis of the reflected light allows one to monitor axial strain or temperature changes[3].

$$\Delta\lambda_B = \lambda_B (1-P)\Delta\varepsilon + \lambda_B \beta \Delta T \qquad (1)$$

In this equation P is the (effective) strain-optic constant and β is the temperature coefficient of the grating. The spectrum of an FBG written in a single mode fibre which has an unloaded Bragg wavelength of 1550nm will shift ± 1,2pm/με and ± 14pm/°C [4].
In sensing applications where only one perturbation is of interest, the deconvolution of temperature and strain becomes necessary.

Real world applications

Before discussing possible applications, some advantages of this type of sensor over classical strain gauges can be noted. The strain and temperature information is encoded into a wavelength which is an absolute parameter. Measurement interruption, by accident or intended, does not cause any problem, and does not ask for a new calibration, as is most often the case with classical strain gauges. In addition, the result does not depend on the total light level; losses in the connecting fibres or optical couplers, or fluctuations in the power of the broadband light source have therefore no influence. This is an important aspect when considering long-term field measurements. Furthermore, the wavelength-encoded nature of the output facilitates wavelength division multiplexing. It allows the distribution of several gratings over a single optical fibre, by assigning each sensor to a different portion of the available spectrum of the light source.

Also thanks to their small size (down to 40µm without coating [5]), corrosion resistance, insensitivity to electromagnetic interference, optical fibres have become more and more widespread in sensor design. Strain [6],[7], Pressure [8],[9] , Temperature[10],[11], hydrogen detection [12] and crack detection sensors [13] are some of the many applications which use FBGs as basic principle. Mostly, they are used in areas (mining industry, aerospace applications, space applications) in which harsh environments make it impossible to use classical sensing principles.

Sensitivity to a multi-axial loading condition

Not only axial strain and temperature causes the Bragg spectrum to shift. Former theoretical calculations and simulations have proven that the spectrum (shape as well as central wavelength) is not only dependent on the axial strain but on the **total strain state** of the optical fibre[14]. This means that transversal strain components have an influence on the Bragg wavelength shift by changing both the length of the grating and the refractive index of the fibre.

Since the current sensor design uses FBGs written in 'High Birefringence'-fibres (HiBi-fibre), the effects of the total strain state on these spectra will be discussed more thoroughly. The birefringence of this type of fibre is generated or, by introducing stress applying parts inside the fibre (e.g. Panda or BowTie-fibre, the latter is the type which will be used in the new sensor design), or by changing the geometry of the fibre (e.g. D-shaped fibre, elliptical cladding fibre). Chehura et al. gives a survey on the relative sensitivities of these different types of fibres.[15]
For this type of fibre, both polarization modes will satisfy the Bragg condition at different wavelengths due to the difference in refractive index of the two polarization axes. Therefore, FBGs written in such fibres will reflect two distinct peaks, one for each polarization axis. The peaks are normally indicated with the names 'fast' and 'slow', corresponding to the propagation speed of light along both polarisation axes of the HiBi-fibre. (see Figure 2)

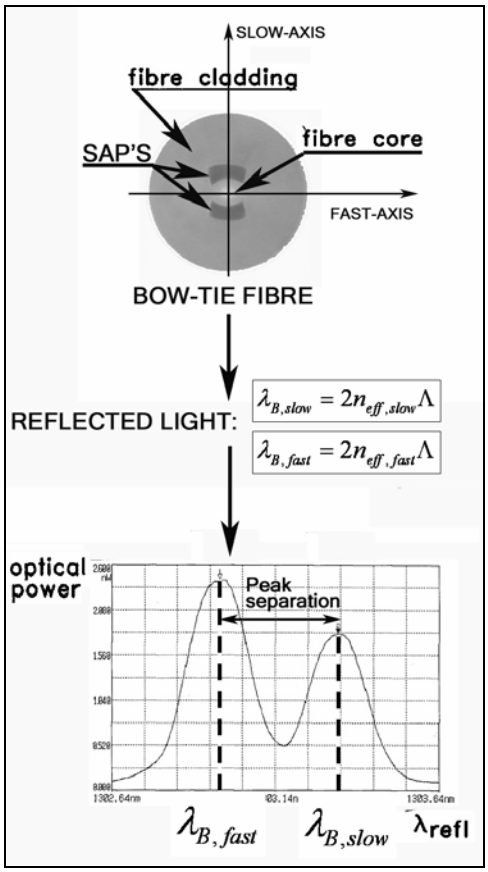

Figure 2 Shown is the typical spectral response from a grating inscribed in a HiBi-fibre after in-coupling of light of a broadband light source. The two polarisation axes of the fibre have different Bragg-resonances due to their different refractive indices. On the left a microscopic picture of a Bow-Tie fibre is included on which the 'Stress Applying Parts' (SAP's) causing the birefringence are marked.

The separation of the two peaks is directly proportional to the birefringence of the fibre. A change in axial strain or temperature will not affect the birefringence of the fibre, but will cause an overall shift of the refractive indices towards higher or lower values. This results in a similar shift in Bragg wavelength for the peaks from both polarization axes, as shown in Figure 3. If on the other hand a change in transversal strain is applied, a change of the birefringence of the fibre will occur and this results in a change of the peak separation, shown in Figure 3 [16]. Depending on the direction of the applied transversal strain with respect to the polarisation axes of the fibre, the peak shift will increase or decrease.

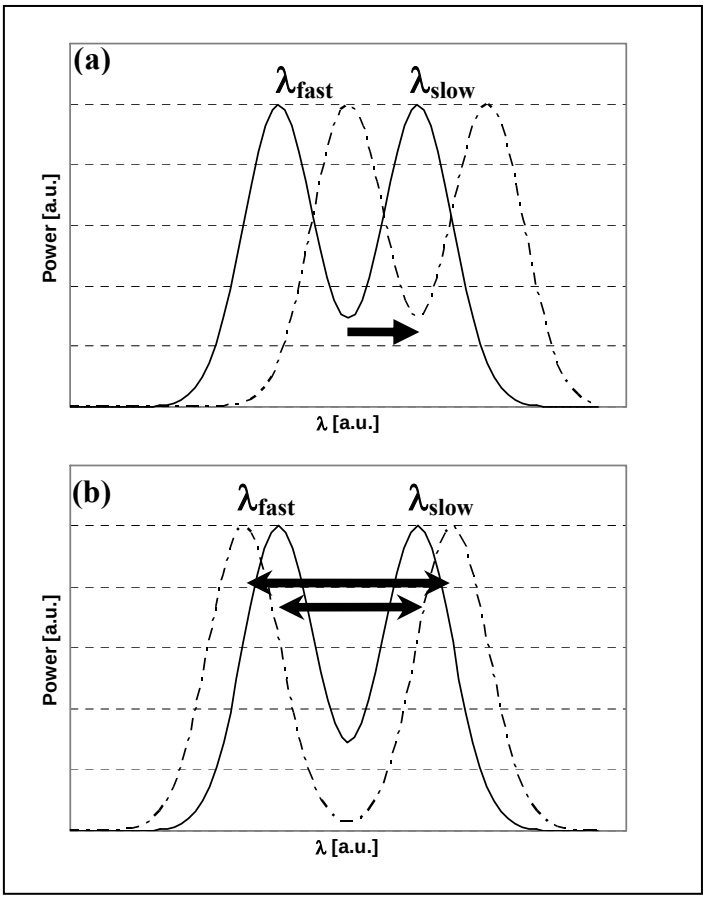

Figure 3 Effect on the spectral response of a HiBi-FBG due to (a) axial stress or uniform temperature change and (b) transverse stress. Original spectrum in full line and resulting spectrum due to the applied load in dashed line.

In general, the fibre will be exposed to both longitudinal and transverse strains and to temperature changes. The corresponding shifts of the fast and slow Bragg wavelengths are given by equation (2)[4].

$$\begin{cases} \dfrac{\Delta\lambda_{slow}}{\lambda_{slow}} = GF1_{\varepsilon,slow}\Delta\varepsilon_{slow} + GF2_{\varepsilon,slow}\Delta\varepsilon_{fast} + GF3_{\varepsilon,slow}\Delta\varepsilon_{axial} + \alpha_{slow}\Delta T \\ \dfrac{\Delta\lambda_{fast}}{\lambda_{fast}} = GF1_{\varepsilon,fast}\Delta\varepsilon_{slow} + GF2_{\varepsilon,fast}\Delta\varepsilon_{fast} + GF3_{\varepsilon,fast}\Delta\varepsilon_{axial} + \alpha_{fast}\Delta T \end{cases} \quad (2)$$

$\Delta\varepsilon_{slow}, \Delta\varepsilon_{fast}, \Delta\varepsilon_{axial}$ are the strains which exist along respectively the slow, the fast and the longitudinal direction of the optical fibre. The GF-coefficients are the so-called gauge factors and are characteristic for the FBG-sensor. These gauge factors are theoretically given by[4]:

$$\begin{cases} GF1_{\varepsilon,slow} = -\frac{n_{slow,eff}^{\ 2}}{2} p_{11} & GF1_{\varepsilon,fast} = -\frac{n_{fast,eff}^{\ 2}}{2} p_{12} \\ GF2_{\varepsilon,slow} = -\frac{n_{slow,eff}^{\ 2}}{2} p_{12} & GF2_{\varepsilon,fast} = -\frac{n_{fast,eff}^{\ 2}}{2} p_{11} \\ GF3_{\varepsilon,slow} = 1 - \frac{n_{slow,eff}^{\ 2}}{2} p_{12} & GF3_{\varepsilon,fast} = 1 - \frac{n_{fast,eff}^{\ 2}}{2} p_{12} \end{cases} \quad \textbf{(3)}$$

In which the p_{11} and p_{12} are the strain-optic constants which where determined for a 'Single Mode Fibre' (SMF-fibre) by Berthold et al.[17]
This type of sensor (FBG inscribed in a HiBi-fibre) enables the measurement of two Bragg-wavelengths and hence yields the potential of determining two strain-components. However, to determine the 3D-strain components $\Delta\varepsilon_x$, $\Delta\varepsilon_y$ and $\Delta\varepsilon_z$ which exist along the main axes of a structure, at least 2 sensors of this type are required. Two sensors would yield 4 measurable wavelengths which theoretically allows the determination of a fourth parameter (e.g. the temperature) as well.

Multi-axial sensor design

By using a second grating written in the same fibre, the set of equations (2) can be extended with two extra equations, leading to a set of four equations with 4 unknown parameters ($\Delta\varepsilon_{slow}$, $\Delta\varepsilon_{fast}$, $\Delta\varepsilon_{axial}$, ΔT). A general representation is given by:

$$\begin{bmatrix} \Delta\lambda_{B1,slow} \\ \Delta\lambda_{B1,fast} \\ \Delta\lambda_{B2,slow} \\ \Delta\lambda_{B2,fast} \end{bmatrix} = K \begin{bmatrix} \Delta\varepsilon_{slow} \\ \Delta\varepsilon_{fast} \\ \Delta\varepsilon_{axial} \\ \Delta T \end{bmatrix} \quad \rightarrow \quad \begin{bmatrix} \Delta\varepsilon_{slow} \\ \Delta\varepsilon_{fast} \\ \Delta\varepsilon_{axial} \\ \Delta T \end{bmatrix} = K^{-1} \begin{bmatrix} \Delta\lambda_{B1,slow} \\ \Delta\lambda_{B1,fast} \\ \Delta\lambda_{B2,slow} \\ \Delta\lambda_{B2,fast} \end{bmatrix} \quad \textbf{(4)}$$

The subscript 1 and 2 in equation (4) corresponds to the first FBG (lower λ_B) and the second FBG (higher λ_B) respectively. Using the matrix formulation on the right it is (theoretically) possible to determine three strain components and the temperature from the four measurements of Bragg wavelength. The K matrix consists of the gauge factors and the temperature coefficients multiplied with four reference Bragg wavelengths (e.g. in the unloaded condition), and can be expressed as:

$$K = \begin{bmatrix} \lambda_{1,slow} & 0 & 0 & 0 \\ 0 & \lambda_{1,fast} & 0 & 0 \\ 0 & 0 & \lambda_{2,slow} & 0 \\ 0 & 0 & 0 & \lambda_{2,fast} \end{bmatrix} \begin{bmatrix} GF1_{\varepsilon,slow\_1} & GF2_{\varepsilon,slow\_1} & GF3_{\varepsilon,slow\_1} & \alpha_{slow\_1} \\ GF1_{\varepsilon,fast\_1} & GF2_{\varepsilon,fast\_1} & GF3_{\varepsilon,fast\_1} & \alpha_{fast\_1} \\ GF1_{\varepsilon,slow\_2} & GF2_{\varepsilon,slow\_2} & GF3_{\varepsilon,slow\_2} & \alpha_{slow\_2} \\ GF1_{\varepsilon,fast\_2} & GF2_{\varepsilon,fast\_2} & GF3_{\varepsilon,fast\_2} & \alpha_{fast\_2} \end{bmatrix} \quad \textbf{(5)}$$

The GF-coefficients of the obtained 4 equations can be determined using a calibration procedure in which transversal and axial strains are varied (this is discussed in the section

'calibration of the sensor'). Similarly, the temperature sensitivity coefficients α_{slow} and α_{fast} can be determined in a temperature calibration procedure.
The possibility of finding a unique solution for matrix equation (4) is strongly dependent on the used sensor configuration. This should be designed such that the different FBGs show a diverse response to the applied strain and temperature; only in this case the four equations will be independent. A number of different designs have been studied and reported in Luyckx et al [18]. For each configuration the condition number of the solution matrix (inverse of the K-matrix, equation (5)) has been analyzed. A high condition number means that the equations are mutually dependent which will lead to large faults in the output (undesirable) for small faults in the input. Very low condition numbers mean that the equations are (almost) independent and the output will consequently be very accurate. By comparing the condition number of the set of equations (4) we could conclude that the capillary design (see the following section) leads to the best discrimination.

Capillary Design

The targeted specifications of the MASSFOS-project for temperature and strain measurements are summarized in
Table 1.

Table 1Targeted specifications for temperature and strain measurements of the MASSFOS-project[2]

Parameter	Value	Unit
Axial strain resolution	5-10	µstrain
Transverse strain resolution	5-10	µstrain
Temperature resolution	1-2	°C
Temperature range	-25 to 170	°C

To keep the resolution of the sensor within the limits stated in
Table 1, it is necessary that the two gratings, used in the new design, have a diverse response on external loading. In our concept we try to reach this goal by decreasing the sensitivity to transverse stress of the second grating. The concept exists of two gratings which are written in the same fibre. The first grating is sensitive to temperature, longitudinal stress as well as transverse stress and the second one only to temperature and longitudinal stress (we try to isolate the transverse stress by using a capillary, see Figure 4). If the temperature sensitivities of the main polarization-axes of the HiBi-fibre are sufficiently different, the peak separation of the second grating will also allow measuring temperature changes [19].
The optical fibre is an 80µm Bow-Tie fibre which has a 37,5 µm thick polyimide coating, in total an outer diameter of 155µm. The capillary exists out of silica tubing coated with polyimide; the inner diameter of this tube is 180µm while the outer diameter is 340 µm. The capillary is slide over the second grating and is sealed at its two ends with silicone to prevent epoxy flow inside the tube.

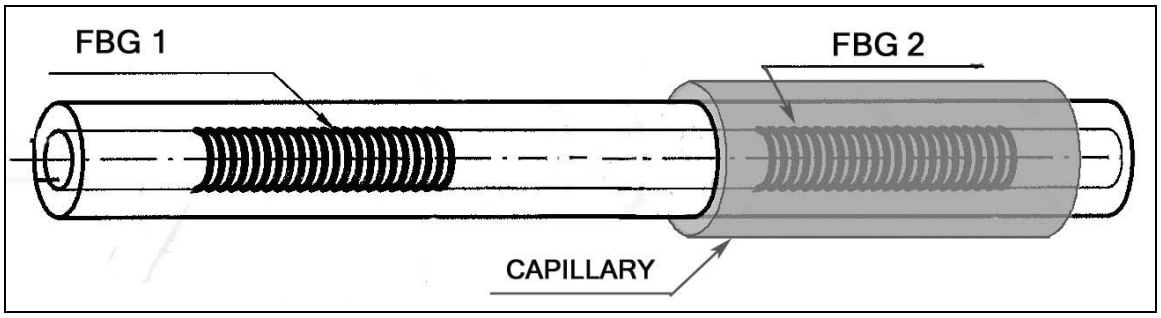

Figure 4 Schematic representation of the new sensor concept. The first grating is embedded in the composite material according to normal procedures. The second grating is put in a capillary which can be embedded into the composite material.

Feasibility of the capillary design

Theoretical accuracy of the sensor

Luyckx et al.[18] calculated the standard deviation of the expected fault on the output by assuming that the wavelengths of the FBGs can be measured with an accuracy of ±1pm. These results are represented in Table 2.

Table 2 Sensitivity analysis for the capillary design

Capillary design	Condition number	Parameter	Error (1pm error)
Strain (3D) + Temp	±100	Transversal Strain ($\Delta\varepsilon_{fast}$)	±9 [με]
		Transversal Strain ($\Delta\varepsilon_{slow}$)	±4 [με]
		Axial Strain ($\Delta\varepsilon_{axial}$)	±25 [με]
		Temperature (ΔT)	±2°C

From this table it can be concluded that each parameter can be calculated within reasonable precision comparable with the resolutions stated in Table 1. For that reason, this sensor configuration has been proposed as the optimal sensor for embedded measurements of more-dimensional strain components.

Calibration of the sensor

When we use equation (4) to determine the total strain state and temperature of the composite laminate, we need three distinct types of calibration to determine all the parameters of the K-matrix (Equation(5)). For characterizing the FBG we used the SpectralEye 600® which is a handheld interrogation system with a wavelength resolution of ±1pm.

TRANVERSE SENSITIVITY

At first, we determine the spectral behaviour of the grating upon **transverse loading** condition with a set-up build at the Ghent University (see Figure 5).

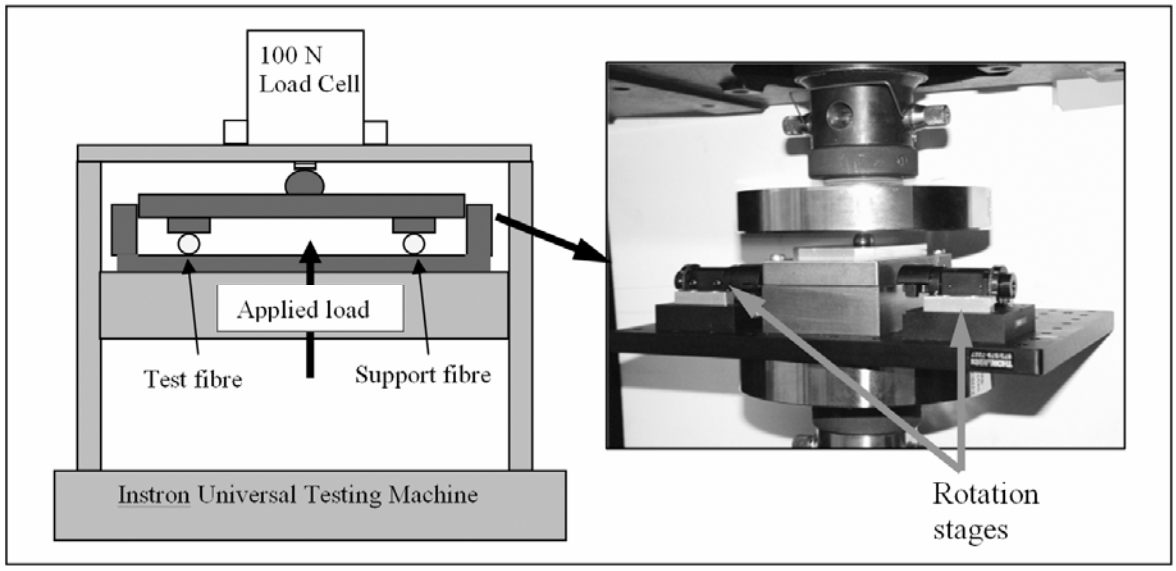

Figure 5 Designed multi-axial FBG calibration setup. Picture of the stress bench realised at UGent. The stress is applied with an Instron 4505 universal materials testing machine

To determine the sensitivity to transverse loading as a function of the orientation of the eigen axes, a pair of rotational stages with high angular resolution (2° angular precision) is required to rotate the grating of the HiBi-fibre. Both the test fibre and a dummy piece of the same fibre type are stripped (over a length of 25mm) and placed parallel to each other and are sandwiched between two plates. The loading fixture is designed to minimize fibre twist during calibration. For each 15° rotation angle of the fibre, from 0 up to 180°, we progressively applied a line load of 0 N/mm up to 1,8 N/mm.
In Figure 6, we present the effect induced by the applied force on the reflection spectra of the slow and the fast axis of the FBG. In the figure the component of the slow axis varies more rapidly than the component of the fast axis which induces an increase in peak separation. For this orientation a sensitivity of 0,1717 nm/(N/mm) can be found for the slow axis, while a smaller sensitivity of 0,0168 nm/(N/mm) can be noted for the fast axis.

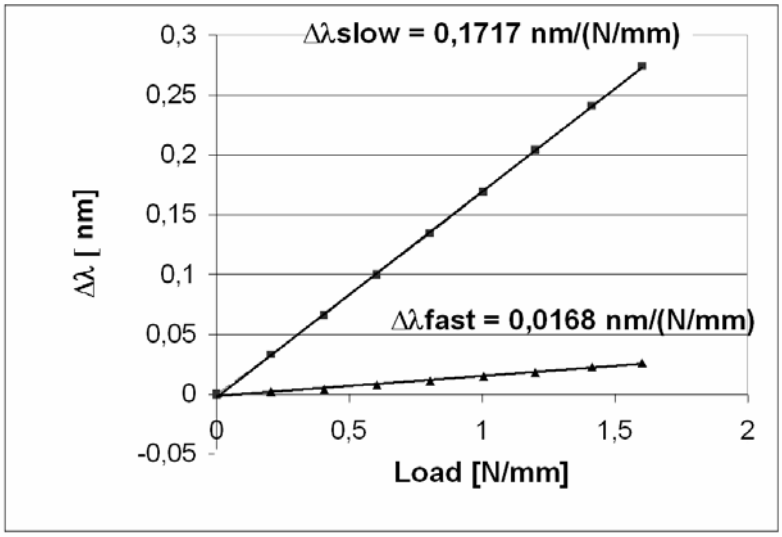

Figure 6: Comparison of the Bragg peak shift for the fast and the slow axes versus the applied load on FBG inscribed in a Bow-Tie fibre for an orientation of 90°.

The same analysis can be repeated for each orientation of the polarization axis of the fibre with respect to the applied load. In Figure 7 the load sensitivities are plotted as a function of the angle of rotation of the HiBi-fibre containing the FBG sensor. Because of symmetry reasons the angle of rotation was varied from 0 to π rad.

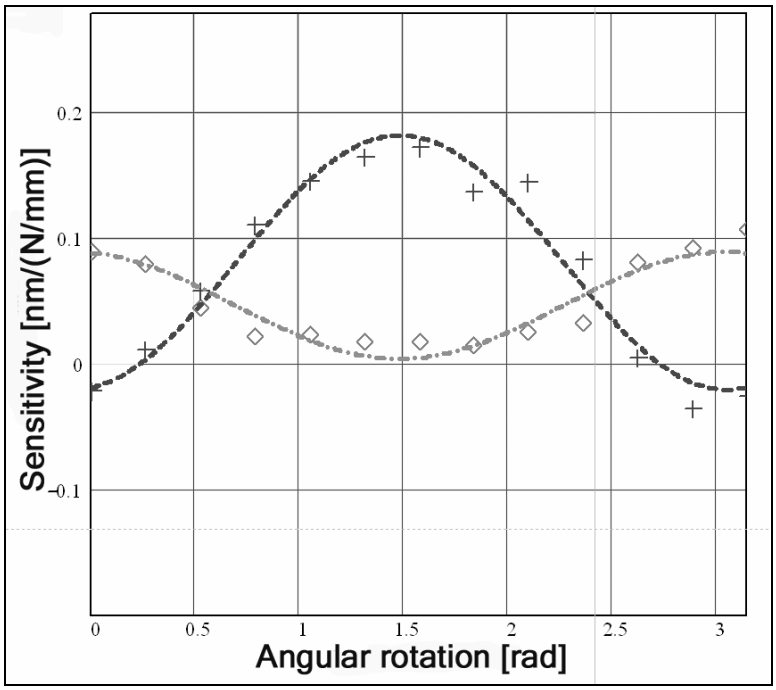

Figure 7: Transverse strain sensitivity versus angle of orientation for FBG in a Bow-Tie Fibre. + = experimental data for the slow axis; □ = experimental data obtained for the fast axis.

The maximum sensitivity for slow and fast axis was obtained when the applied load was oriented along the respective optical eigen axis of the fibre. The minimum sensitivity, in

contrast, was found when the applied load was rotated by an angle of 90° with respect to the respective eigen axis. When the force is applied along the slow axis, the induced stress adds to the internal stress of the stress bars (SAPs) of the BowTie fibre. This causes an increase of the birefringence of the fibre and hence an increase of the peak separation as well. The opposite effect was observed when the stress was applied along the fast axis of the fibre. The peak separation decreases progressively up to merging of the peaks. This phenomenon is also linked to the birefringence of the fibre. When the force is applied along the fast axis of the fibre, the stress along the fast axis compensates progressively the induced slow axis internal stress bars effect. The birefringence of the fibre decreases progressively and consequently the peak separation decreases. Similar values were found by Chehura et al.[15]

By using the curves in Figure 7, and knowing that the applied line load causes stress along both the eigen axes[20], we can now determine the gauge factors of equation 5 through decoupling of the two curves (Table 3).

Table 3 Values of the gauge factors

$GF1_{\varepsilon,slow}$	-0,42253	$GF1_{\varepsilon,fast}$	-0,1215
$GF2_{\varepsilon,slow}$	-0,1757	$GF2_{\varepsilon,fast}$	-0,2253

AXIAL SENSITIVITY

Secondly, the axial gauge factor can be found using a simple tensile experiment. The principle of this experiment is to submit the FBG to different force intensities and to measure the corresponding Bragg wavelength shift. In the set up (Figure 8) the grating is loaded by means of calibrated weights. In the calibration experiment the longitudinal strain is given by:

$$\varepsilon = \frac{F}{ES} \qquad (6)$$

Where E is the Young modulus of the fibre 72,9 GPa ; S is the transversal section of the fibre; and F is the applied force .

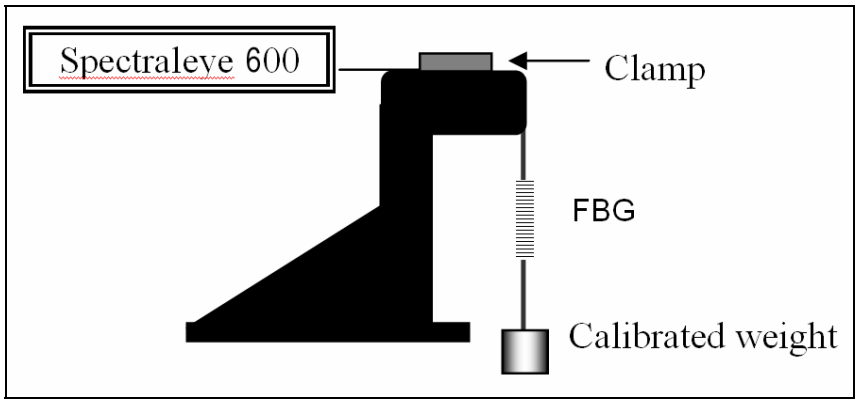

Figure 8: Experimental setup for longitudinal strain measurement.

For each applied force on the FBG, we registered the response via the SpectralEye 600. After plotting the curve of λ_B versus ε_3 we determined the longitudinal strain sensitivity from the slope of the curve by least squares fitting (Figure 9).

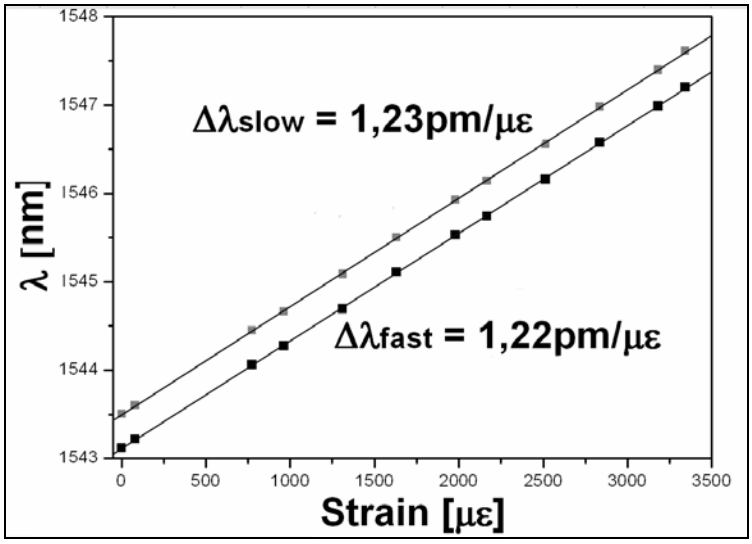

Figure 9: Longitudinal strain dependence of λ_B for the slow and the fast axis.

By axially straining the fibre, some transverse strains are induced due to the Poisson's coefficient of the fibre material. Therefore it is necessary to decouple longitudinal strain from the transversal strain components. This can be done by using the transverse gauge factors written in Table 3.

Table 4 Values of the gauge factors

$GF3_{\varepsilon,slow}$	0,6946	$GF3_{\varepsilon,fast}$	0,7311

The values found in Table 4 are similar with the value of the strain optic constant (*P*) of equation (1). Though, a difference exists between the gauge factor of the slow and the fast axis. This creates the possibility of using the grating inside the capillary to decouple axial strain from temperature.

THERMAL SENSITIVITY

Finally, a temperature calibration was performed using a climatic chamber. The temperature was varied from 0°C up to 100°C. For each FBG we measured the temperature dependence of the Bragg wavelength (λ_B) from which we could determine the FBG fast and slow axis sensitivities from the slope on the graphs (see Figure 10). We can see that the slow and fast axis sensitivities are slightly different for each FBG. The difference in sensitivity between fast and slow axis is ±0.4 pm/°C.

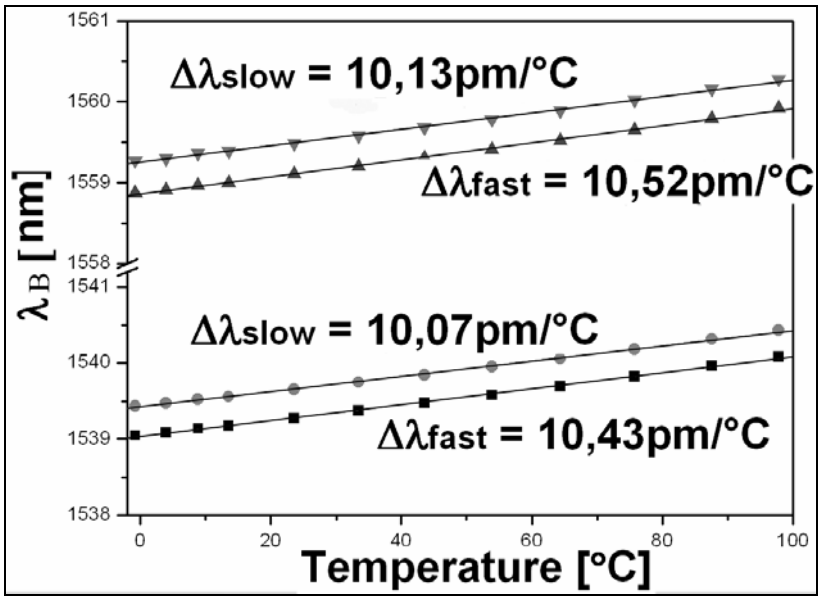

Figure 10: Temperature dependence of λ_B for the BowTie fibre. The temperature sensitivities for the fast and slow axis of the two FBGs are indicated on the graph.

By altering the temperature, longitudinal as well a transversal strains are induced in the fibre, due to the thermal expansion coefficient of the optical fibre. This means that it is only possible to determine the temperature gauge factor (α_{slow} and α_{fast}) when both the longitudinal as well as the transversal strain influences are canceled out of the measured data in Figure 10. In Table 5 the thermal gauge factors are noted: they are similar with the ones that can be found for uni-axial FBGs.[4]

Table 5 Values of the gauge factors dependent on temperature

α_{slow}	$6{,}52*10^{-6}$ 1/K	α_{fast}	$6{,}58*10^{-6}$ 1/K

Again a small difference exists between the gauge factors of the slow and the fast axis which creates the possibility of using the grating inside the capillary to decouple axial strain from temperature.

Experimental accuracy of the sensor

By using the gauge factors depicted in Table 3-5 the standard deviation of the expected fault on the output can be calculated, by assuming that the wavelengths of the FBGs can be measured with an accuracy of ±1pm. These results are represented in Table 6.

Table 6 Sensitivity analysis for the capillary design

Capillary design	Condition number	Parameter	Error (1pm error)
Strain (3D) + Temp	±16	Transversal Strain ($\Delta\varepsilon_{fast}$)	±4,6 [με]
		Transversal Strain ($\Delta\varepsilon_{slow}$)	±2,5 [με]
		Axial Strain ($\Delta\varepsilon_{axial}$)	±1 [με]
		Temperature (ΔT)	±1°C

In this table the resolution of the axial strain component is a lot better than theoretically expected (Table 2) due to the diverse response of the slow and the fast axis upon axial strain and temperature change.

Preliminary feasibility study of embedded sensors in thermo hardened composite elements

One of the important things, when using the capillary design as embedded sensor, is to check its sensitivity towards transverse loading. The first grating, inside the capillary, should be insensitive to this type of loading. Experiments have been conducted in which a composite laminate with embedded sensor has been subjected to a transverse loading condition. The obtained results are illustrated in Figure 11:

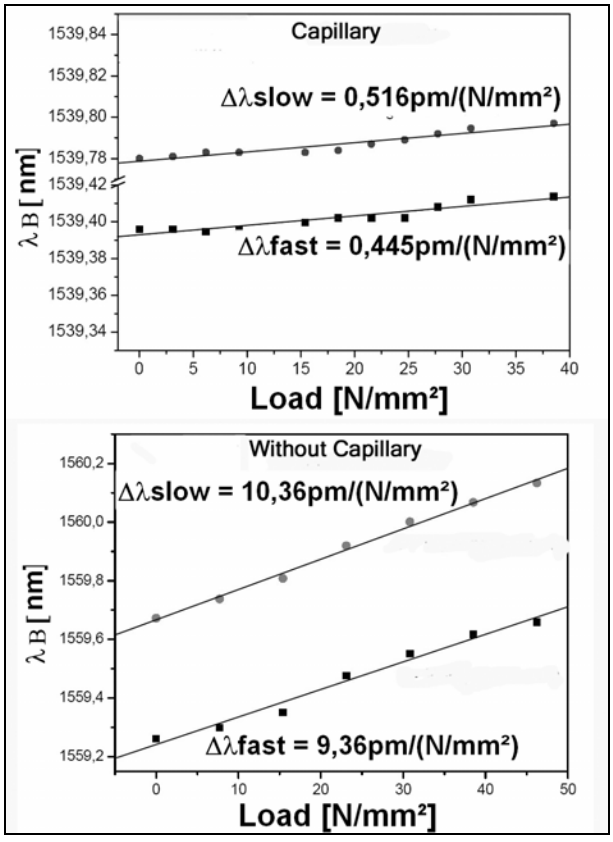

Figure 11 The sensitivity to transverse stress of the capillary design. Left side: sensitivity of the FBG embedded in the capillary, right side: sensitivity of the second FBG.

Due to pure transverse loading only a small effect is noticed on the spectrum of the grating inside the capillary (Figure 11), while on the other grating a clear linear movement of the spectrum can be noticed. The small dependency of the grating inside the capillary is due to the elongation of the laminate (resulting from the Poisson coefficient).

Another requirement, in contrast with transverse loading, is that both gratings should have a comparable sensitivity to longitudinal tension. This means that the axially applied stress must be transferred onto the grating embedded in the capillary. These results are presented in
Figure 12.

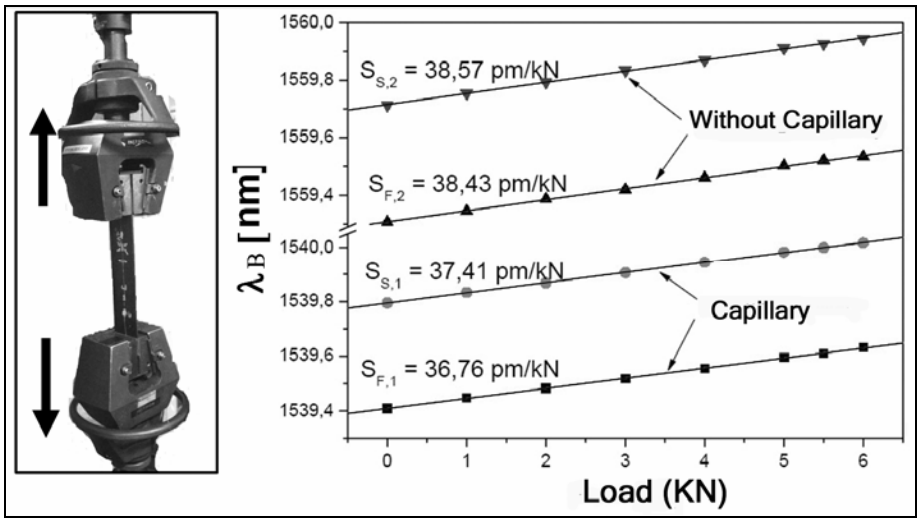

Figure 12 Left: indication of the direction of the applied load. Right: the sensitivity to longitudinal stress of the capillary design embedded in a thermo hardened composite sample.

Because the magnitude of the Bragg-peak shift is quasi the same (Figure 12), we can conclude that there is a good transfer of longitudinal strain of the composite on the first as well as on the second grating. However the small difference which exists between the sensitivity of the two gratings needs closer study.

Also temperature calibration experiments were conducted to complete the feasibility study of this sensor design (see Figure 13). However, by increasing the temperature also multi-axial strains are induced inside the composite sample. This strains are induced due the expansion of the composite material but also due to the difference between the thermal expansion coefficient of the sensor (glass fibre) and the material (carbon-epoxy laminate). Further research on this matter is needed.

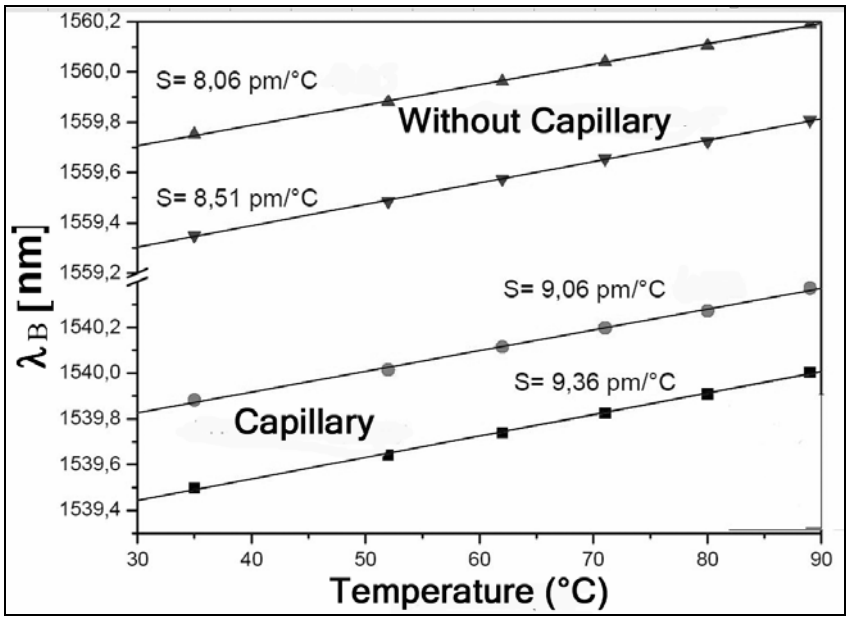

Figure 13 Temperature sensitivity of the capillary design embedded in a thermo hardened composite test sample.

Conclusions

It has widely been proven that fibre Bragg gratings can be used as a very reliable monitoring system for the measurement of axial strains in composite elements. However, when damage or inter-laminar strains/stresses need to be measured this type of sensor does not provide sufficient information. In that case we can switch to multi-axial fibre Bragg gratings which are sensitive to longitudinal as well as transversal strain/stress.
A new sensor design was presented which uses a capillary to enhance the strain resolutions. The theoretical resolutions were acceptable with respect to other monitoring principles. Two assumptions were made to obtain these resolutions (ie. the grating inside the capillary is insensitive to transverse stress, but remains sensitive to axial stress). Some experiments (tensile and transverse pressure tests) were conducted to prove the feasibility of the sensor. (Tensile and a pressure test)
By calibrating the sensor we succeeded in determining the experimental strain resolution ($\Delta\varepsilon_{fast}$= ±4,6 μstrain, $\Delta\varepsilon_{slow}$= ±2,5μstrain , $\Delta\varepsilon_{axial}$= ±1μstrain) and the temperature resolution (ΔT= ±1°C). This last aspect could become an interesting topic in replacing temperature compensation when using fibre Bragg gratings.

Acknowledgements

The authors would like to acknowledge the financial support of the European Space Agency (Contract No. 19026/05/NL/IA). Special thanks go to Iain McKenzie and Andreas Obst working at ESA for their critical but positive input. The authors also like to thank their partners in this project, FOS&S (Belgium) and XenIC's (Belgium), for the material support.

References

(1) CC Hiel, M Sumich, and D P Chappell,"A curved beam test specimen for determining the interlaminar tensile strength of a laminated composite, Journal of composite materials, vol 25, pp 854-868, July 1991.

(2) J Vlekken, J Degrieck, J Vermeiren, "Multi-axial stress and strain sensing of thermo hardened composite elements using Fibre optic sensors", full proposal, ESA-contract 19026/05/NL/I , (2005), internal document.

(3) CD Butter and GB Hocker, "Fibre optics strain gauge." Applied Optics 17, nr.18 1978.

(4) W De Waele, "Structural monitoring of composite elements using optical fibres with Bragg-sensors." PHD thesis at Ghent University, 2001-2002

(5) N Takeda, Y Okabe, Y Kuwahara, S Kojima, T Ogisu, "Development of smart composite structures with small-diameter fibre Bragg grating sensors for damage detection: Quantitative evaluation of delamination length in CFRP-laminates using Lamb wave sensing", Composites Science and Technology vol. 65, pp2575-2587, 2005

(6) W De Waele, J Degrieck, R Baets, W Moerman and L Taerwe, "Load and deformation monitoring of composite pressure vessels by means of optical fibre sensors", Insight, vol. 43, No8, August 2001

(7) J Degrieck, W De Waele, P Verleysen, "Monitoring of fibre reinforced composites with embedded optical fibre Bragg sensors, with application to filament wound pressure vessels", NDT&E international, vol.34,pp289-296, 2001.

(8) MG Xu, H Geiger, JP Dakin, "Fibre grating pressure sensor with enhanced sensitivity using a glass-bubble housing", Electronics Letters, vol. 32, No2, Jan 1996.

(9) PM Nellen, P Mauron, A Frank, U Sennhauser, K Boknert, P Pequignot, P Bodor and H Brandle, "Reliability of fiber Bragg grating based sensors for downhole applications", Sensors and Actuators A-Physical, vol. 103, No 3, pp364-376, Feb 2003.

(10) UC Mueller, L Raffaelli, A Reutlinger, I Latka, W Ecke, G Tumino and H Baier, "Integration and Operation of fiber Optic Sensors in Cryogenic Composite Tank structures", Proceedings of SHMII, Munich, pp1270-1277, July 2004

(11) SL Tsao and JS Wu, “Highly accurate temperature sensor using two fiber Bragg gratings, IEEE Journal of selected topics in quantum electronics, vol. 2, No4, pp 894-897, Dec 1996.
(12) M Consales, S Campopiano, A Cutolo, M Penza, P Aversa, G Cassano, M Giordano, A Güemes and A Cusano, « Carbon Nanotubes-Based optical sensor for hydrogen detection at cryogenic temperature, Proceedings of SHMIII, Granada, pp898-905, July 2006.
(13) Y Okabe, R Tsuji, N Takeda, “Applicition of chirped fiber Bragg grating sensors for identification of crack locations in composites”, Composites Part A: applied science and manufacturing, vol. 35, pp 59-65, 2003
(14) G Luyckx., W De Waele, J Degrieck, “Multi-axial stress and strain sensing with Bragg-sensors: a theoretical study”, proceedings ACOMEN 2005, Ghent, 2005
(15) E Chehura, CC Ye, S E Staines, S W James, R P Tatam,”Characterization of the response of fibre Bragg gratings fabricated in stress and geometrically induced high birefringence fibres to temperature and transverse load”, Smart Materials and structures, no13, pp888-895, 2004
(16) G Luyckx, J Degrieck, W De Waele, W Van Paepegem,J Van Roosbroeck, K Chah, J Vlekken, I Mc Kenzie, A Obst, “Feasibility study on measuring axial and transverse stress/strain components in composite materials using Bragg sensors”, Proceedings of ICSO, Noordwijk, June 2006.
(17) A Bertholds, R Dändliker, ”Determination of the Individual Strain-Optic Coefficients in Single-Mode Optical Fibres.” Journal of Lightwave Technology 6, No 1 (1988) pp. 17-20.
(18) G Luyckx, W De Waele, J Degrieck, J Vlekken, K Chah. “Multi-axial Fiber Bragg sensors for monitoring purposes”, Conference proceeding ECCM12, Biarritz. August 2006.
(19) J Vlekken, W De Waele, J Vermeiren, “Multi-axial stress and strain sensing with Fibre optic sensors”, Critical design report, ESA-contract 19026/05/NL/I , (2005), internal document.
(20) R Wagreich, W. Atia, H Singh, and J Sirkis, « effects of diametric load on fibre Bragg gratings fabricated in low birefringent fibre », Elctronics letters, vol 32, no13, pp1223-1224,1996